Biophysical Journal Volume 73 July 1997 52–66

A Model of the Nicotinic Receptor Extracellular Domain Based on Sequence Identity and Residue Location

Igor Tsigelny,* Naoya Sugiyama,* Steven M. Sine,# and Palmer Taylor*
*Department of Pharmacology, University of California, San Diego, La Jolla, California 92093-0636, and #Receptor Biology Laboratory, Mayo Clinic and Foundation, Rochester, Minnesota 55905 USA

ABSTRACT We have modeled the extracellular domains of individual subunits (amino acids 31–200) in the nicotinic acetylcholine receptor using sequence homology with copper binding proteins of known crystal structure, plastocyanin and pseudoazurin, and data from recent site-specific mutagenesis, antibody mapping, and site-directed labeling studies. These data formed an initial model that was refined using molecular dynamics and mechanics as well as electrostatic and solvation energy calculations. The sequences between residues 31 and 164 in the α_1-subunit and corresponding residues in homologous receptor subunits show similarity with the core sequence of the cation binding site in plastocyanin and pseudoazurin, a region in the template proteins characterized by multiple hairpin loops. In addition to defining the subunit interfaces that comprise the site for agonist and competitive antagonist binding in more detail, the findings show that negatively charged residues cluster in domains arranged to diminish electrostatic free energy of the complex. Electrostatic factors also appear to distinguish the ligand binding interfaces, $\alpha\gamma$ and $\alpha\delta$, from the other three interfaces on the pentameric receptor.

INTRODUCTION

The nicotinic acetylcholine receptor (nAChR) in skeletal muscle is a pentamer of four homologous subunits with a composition of $\alpha_2\beta\gamma\delta$ (cf. Changeux, 1995; Karlin and Akabas, 1995). The subunits share common features of sequence and an amino acid identity ranging between 29 and 52%. The amino-terminal 213 amino acids in each subunit are believed to form the bulk of the extracellular domain, which is followed by the first of four transmembrane domains (M1–M4). The region between M3 and M4 constitutes most of the cytoplasmic mass, whereas the extracellular region between M2 and M3 and the sequence at the very carboxyl-terminus following M4 make relatively small contributions to the mass of the extracellular domain.

Substantial evidence has accumulated to show that the five subunits are assembled around an axis of pseudosymmetry. The axis defines a central channel whose permeability is gated by the binding of acetylcholine and other agonists. Within this assembly are two binding sites for acetylcholine formed at interfaces between subunits. Of the five subunit interfaces, only the $\alpha\gamma$ and $\alpha\delta$ interfaces form high-affinity binding sites for agonists and competitive antagonists (Blount and Merlie, 1989; Sine and Claudio, 1991).

The identification of amino acids contributing to the binding site at the subunit interface was initiated by site-directed labeling with agonists and antagonists (Kao et al., 1984; Dennis et al., 1988; Abramson et al., 1989; Galzi et al., 1990; Middleton and Cohen, 1991; Czajkowski and Karlin, 1995). Site-specific mutagenesis then identified candidate residues in the ligand binding site and established that differences in binding affinity arise from particular residues in the γ- and δ-subunits (Tomaselli et al., 1991; O'Leary and White, 1992; Sine, 1993; Sine et al., 1994; Aylwin and White, 1994; O'Leary et al., 1994; Sine et al., 1995; Sugiyama et al., 1996). Mutagenesis studies have also revealed residues important for subunit assembly (Gu et al., 1991; Kreienkamp et al., 1995; Sugiyama et al., 1996).

With 20 distinct hydrophobic domains projected to span the membrane in the pentameric receptor of 280,000 Da, analysis of this structure at atomic resolution is limited by formation of crystals of the pentameric receptor suitable for x-ray diffraction. Thus, other means have been sought to obtain details of the receptor structure. Electron microscopy reconstruction has provided an elegant analysis of the shape of the molecule and identified the positions of some helical regions (Unwin, 1993, 1996). Moreover, visualization of mAb35 bound to the nAChR in tubular crystals has positioned the main immunogenic region at the top of the molecule when viewed from the synaptic face (Beroukhim and Unwin, 1995).

The nAChR from skeletal muscle serves as the prototype for analyzing structure of the family of ligand-gated channels. Included in the family are nAChR from neurons, γ-aminobutyric acid (GABA), glycine, and 5-hydroxytryptamine type 3 (5HT-3), receptors (cf. Changeux, 1995; Karlin and Akabas, 1995). The receptors for excitatory amino acids (i.e., glutamate) appear to be more distant relatives, as the positions of membrane spanning sequences

Received for publication 6 January 1997 and in final form 3 April 1997.

Address reprint requests to Dr. Palmer Taylor, Department of Pharmacology, University of California, San Diego, La Jolla, CA 92093-0636. Tel.: 619-534-1366; Fax: 619-534-8248; E-mail: pwtaylor@ucsd.edu.

Coordinates will be submitted to the Protein Data Bank in Brookhaven. They may be requested through itsigeln@ucsd.edu.

Dr. Naoya Sugiyama is a visiting scholar from Yokohama City University, Yokohama, Japan.

0006-3495/97/07/52/15 $2.00

within the linear sequence and location of the ligand binding site differ greatly from the nicotinic receptor superfamily. In the case of excitatory amino acid receptors, a bacterial binding protein for glutamate homologous in sequence to the glutamate receptor has been crystallized, thereby providing a suitable template for analyzing receptor structure (O'Hara et al., 1993; Stern-Bach et al., 1994, Sutcliffe et al., 1996).

The now-extensive chemical labeling, antibody recognition, and site-specific mutagenesis studies on the nicotinic receptor family have yielded useful information on the probable positions of certain amino acid side chains. Moreover, we find sequence homology of limited segments of the nicotinic receptor subunits with a family of proteins of known crystal structure. We combine this information to construct a template to serve as a working model for the structure of the extracellular portion of the nAChR.

METHODS

Sequence alignment

We used a double window alignment of query and template sequences for the candidate protein families. As emphasized previously (Fitch, 1966), using a too-long query sequence may preclude finding the appropriate regions of identity, whereas a sequence that is too short may prove misleading by creating excessive gaps in potential regions of homology. Doolittle (1990) pointed out that the use of shorter query sequences in some cases reveals significant homology, whereas a long query gives low similarity in sequence alignments. The moving window procedure has also been applied to multiple members of families of DNA sequence to establish a consistency of pattern (Hultner et al., 1994).

In our procedure we have used query sequences of 45–55 amino acids and 90–105 amino acids. They were moved one residue at a time over template sequences of comparable length. Thus, all possible positions of the query and template sequences are compared and regions of nonidentity serve to control the method internally. The FASTA program (Pearson and Lipman, 1988; Pearson, 1996) with *codaa* matrix (gap penalty −12/−4) was used in our sequence comparison.

The matching of sequences subsequently used segments in the ranges of 50 and 100 amino acids for pairwise alignments between and within a family of five copper binding proteins and the superfamily of subunits of nAChR. Upon completion of the pairwise alignments, a multiple alignment of the copper-binding and nAChR families of proteins was developed.

Modeling of tertiary structures

The crystallographic structures of pseudoazurine precursor (Adman et al., 1989) and plastocyanin (Guss and Freeman, 1983) were structurally superimposed and the aligned sequences from the tertiary structures were compared with the alignment by the double window approach. The amino acid sequences of five small copper-containing proteins [pseudoazurine, pseudoazurine precursor (cupredoxin), plastocyanin, auracyanin, and rusticyanin from *Thiobacillus ferroxidants*] (Nunzi et al., 1993), were used in the sequence analysis and modeling with the sequences of α_1-, α_3-, α_4-, β_1-, γ-, and δ-subunits of the nAChR.

Homology modeling of the nAChR subunits

Regions of the copper binding proteins conserved on the basis of sequence alignment were used as the backbone of the model. Nonconserved regions, found either as inserts or as amino- and carboxyl-terminal extensions from the conserved sequence, were identified. Probable conformations of these regions were constructed using PDB database scanning with the program *Homology* (MSI). Chemical labeling and the influence of site-directed mutagenesis on ligand binding and subunit assembly were subsequently used to orient sets of identifiable residues to particular subunit interfaces and position them with respect to each other. The structures were then relaxed by unrestrained molecular mechanics minimization. A simulated annealing procedure followed by energy minimization was conducted in vacuo to eliminate close contacts in the structure. The program *Discover* (MSI) was used for the annealing and energy minimization calculations.

Electrostatic free energy calculations

Electrostatic fields were calculated by solving the linearized Poisson-Boltzmann equation using the program DelPhi 2.5 (Gilson and Honig, 1988) (MSI). The dielectric constants of the solvent and the protein interior were set at 80 and 4, respectively; the ionic strength was equivalent to 0.145 M NaCl. The Poisson-Boltzmann equation was solved numerically on a 0.9-Å grid. The ionizable residues Glu, Arg, Lys, and Asp were assigned the full charge expected for pH 7, while the His residues were assigned a positive charge of 0.5. The Amber partial charge distribution (Weiner et al., 1984) was used to place partial charges on all atoms in the system. Total electrostatic energies of individual subunits, pairs of subunits, and the pentameric receptor were calculated as a sum of the solvent interaction and the Coulombic energy terms as described by Gilson and Honig (1988).

Experimental results used in modeling

Table 1 lists the residues used in the modeling considerations. Data are compiled from extensive studies conducted by several groups over the past two decades.

Ligand binding sites at subunit interfaces

Expression of different combinations of subunits, affinity labeling, and mutagenesis studies have established that the two ligand binding sites are formed by pairs of subunits: $\alpha\gamma$ and $\alpha\delta$ (Blount and Merlie, 1989; Sine and Claudio, 1991; Gu et al., 1991; Kreienkamp et al., 1995; but also see Unwin, 1996). The γ- and δ-subunits are required for acquisition of a binding site conformation with a ligand affinity and selectivity seen in the intact receptor. Identification of residues labeled by site-specific reagents, residues conferring ligand selectivity for the $\alpha\gamma$ and $\alpha\delta$ sites, and residues governing subunit assembly has led to the concept that equivalent residues in the linear sequence in each subunit map to the same spatial position at one of the two faces of the subunit, which we term the (+), or counterclockwise, and (−), or clockwise faces (Kreienkamp et al., 1995; Sine et al., 1995; Machold et al., 1995).

Residues at the (+) face of the α-subunit

Site-specific labeling and mutagenesis studies have identified three distinct regions in the extracellular domain of the α-subunit that contribute to the ligand binding interface: the region containing Y93, a residue labeled by acetylcholine mustard and nicotine (Cohen et al., 1991), and (*N,N*)-dimethylaminobenzene diazonium fluoroborate (DDF) (Galzi et al., 1990); the region containing W149 and Y151 labeled by DDF (Dennis et al., 1988), and the larger region containing Y190 labeled by lophotoxin (Abramson et al., 1989), C192 and C193 labeled by maleimidobenzyltrimethyl ammonium (MBTA) (Kao et al., 1984), and Y190 and Y198 labeled by DDF (Dennis et al., 1988). Site-directed mutagenesis studies confirmed the contributions to ligand binding affinity of key residues in each of these regions (Tomaselli et al., 1991; O'Leary et al., 1992; Sine et al., 1994; Sugiyama et al., 1996). Equivalent positioning of each subunit in the fivefold pseudo-symmetric pentamer implies a comparable location of the equivalent residues in these three regions at the (+) face.

TABLE 1 Residue positions based on site-directed labeling and mutagenesis studies

Subunits/Residues	Location	Experimental Approaches	Reference
α			
Y93, W149–Y151, Y190–(C192–193)–Y198	(+)*	affinity labeling	Kao et al. (1984); Dennis et al. (1988); Galzi et al. (1990); Abramson et al. (1989)
Y93, W149–Y151, Y190–(C192–193)–Y198	(+)	site-directed mutagenesis	Aylwin and White (1994); O'Leary et al. (1994); Sine et al. (1994); Fu and Sine (1994); Nowak et al. (1995); Tomaselli et al. (1991)
D152–S154	(+)	subunit assembly	Sugiyama et al. (1996)
67–76	MIR, top of extracellular domain	electron microscopy	Beroukhim and Unwin (1995)
γ			
K34	(−)	site-directed mutagenesis	Sine et al. (1995)
W55, E57	(−)	labeling; site-directed mutagenesis	Chiara and Cohen (1992); Prince and Sine (1996)
S111	(−)	site-directed mutagenesis	Sine et al. (1995)
Y117	(−)	site-directed mutagenesis	Sine (1993); Fu and Sine (1994)
I145, T150	(+)	subunit assembly, site-directed mutagenesis	Kreienkamp et al. (1995)
F172	(−)	site-directed mutagenesis	Sine et al. (1995); Prince and Sine (1996)
D174	(−)	cross-linking	Czajkowski et al. (1993)
δ			
S36	(−)	site-directed mutagenesis	Sine et al. (1995); Prince and Sine (1996)
W57, D59	(−)	Affinity labeling [^{3}H] dTC, site-directed mutagenesis	Chiara and Cohen (1992); Prince and Sine (1996)
Y113, T119	(−)	site-directed mutagenesis	Sine et al. (1995)
K147, K152	(+)	subunit assembly, site-directed mutagenesis	Kreienkamp et al. (1995)
I178	(−)	site-directed mutagenesis	Sine et al. (1995); Prince and Sine (1996)
D180	(−)	cross-linking	Czajkowski et al. (1993); Czajkowski and Karlin (1995)
ε			
S106, Y115	(−)	subunit assembly, site-directed mutagenesis	Gu et al. (1991)
P121	(−)	natural mutation	Ohno et al. (1996)
β			
R117	(−)	subunit assembly, site-directed mutagenesis	Kreienkamp et al. (1995)

(+), counterclockwise face; (−), clockwise face.

Residues at the (−) face of the γ- and δ-subunits

Studies of the site-selective ligands, *d*-tubocurarine and α-conotoxin M1, identified four regions of the extracellular domain of the γ- and δ-subunits that contribute to the (−) face of the binding site: two amino-terminal regions, a predisulfide, and a postdisulfide region. The most amino-terminal region contains the residue pair γK34/δS36, which interacts with the postdisulfide determinant to contribute to α-conotoxin M1 selectivity (Sine et al., 1995); subsequent studies showed these residues also contribute to ACh selectivity (Sine and Prince, 1996).

Photolabeling by *d*-tubocurarine indicated a second amino-terminal region contributing to the (−) face γW55/δW57 (Chiara and Cohen, 1992). Subsequent mutagenesis studies showed contributions of equivalent tryptophans in the homomeric, nicotinic α_7, and 5HT-3 receptors to ligand affinity (Corringer et al., 1995). Also within this region is the pair γD57/δE59, which contributes to ACh selectivity (Prince and Sine, 1996).

The predisulfide region is just amino-terminal to the ubiquitous disulfide loop and contains γS111/δY113, which contributes to α-conotoxin M1 selectivity, and γY117/δT118, which contributes to *d*-tubocurarine selectivity (Sine, 1993; Sine et al., 1995). The predisulfide region also includes the invariant P121 that contributes to ACh affinity and is crucial for rapid opening of the channel (Ohno et al., 1996). The postdisulfide region contains γF172/δI178, which contributes to α-conotoxin M1 as well as ACh selectivity (Sine et al., 1995; Prince and Sine, 1996). Also included in the postdisulfide region is the pair γD174/δD180, which was identified by chemical cross-linking to be within 9 Å of αC192/C193 of the α-subunit (Czajkowski and Karlin, 1991, 1995).

Residues influencing subunit assembly

Site-directed mutants that alter the assembly of individual nAChR subunits have also been used to localize key residues to either the (−) or (+) faces of subunits. εS106 and εY115, which correspond to γC106 and δC115, have been assigned to the (−) face, from the results of Gu et al. (1991). βR117 was localized to the (−) face in the β-subunit, and γI145/δK147 and γT150/δK152 were localized to the (+) face of the γ- or δ-subunits by Kreienkamp et al. (1995) on the basis of preferential assembly of subunits. An anionic residue, αD152, also is involved in subunit interactions at the (+) face of the α-subunit because the αD152N mutation and the double mutant α(D152N and S154A) markedly diminish the efficiency of assembly of αγ and αδ dimers (Sugiyama et al., 1996).

Antibody binding site

Recent electron microscopy analysis by Beroukhim and Unwin (1995) established that the MIR, whose epitope is formed by residues 67 to 76 in the α-subunit, is located at an apical position distal to the membrane.

RESULTS AND DISCUSSION

Sequence alignments and tertiary structure of copper binding template proteins

Our initial screens of sequence identity showed similarity between a region of the nAChR subunits and a family of copper binding proteins. Since the tertiary structures of members of the latter family are known, they provide a template for analysis of nAChR structure.

Fig. 1 shows alignments of sequences within the copper binding family using the correspondence of tertiary structures (Fig. 1 *a*) and primary structures (Fig. 1, *b* and *c*). Alignment of the residues that superimpose in the crystal structures of plastocyanin (PCY0) and pseudoazurin (PAZ0) is shown in Fig. 1 *a*. The alignment extends from residue 6 to 105 in plastocyanin and from residue 24 to 143 in pseudoazurin. Fig. 2 shows the positional correspondence of the peptide backbones in the region obtained from the two crystal structures. Despite the relatively low sequence identity of these two proteins in this region, the similarity in tertiary structures is surprisingly close. Three hairpin loops with their tips on both faces of the protein are featured in the two structures.

The FASTA alignments in Fig. 1, *b* and *c* are based solely on primary structures. These alignments within the copper binding family show the greatest sequence identity between related molecules, pseudoazurin 1 (PAZ1), and the plastocyanin precursor 1 (PCY1). Low identity (20.4%) and high global alignment scores (48) are found for an internal region of 48 amino acids, whereas increasing the query and template sequences of this region to 92 amino acids and 102 amino acids (Fig. 1 *c*) increases the residue identity (30.2%) and alignment score (96).

Fig. 3, *a* and *b* shows the double window FASTA alignments using 92 and 102 or 48 and 54 residues of pseudoazurin and plastocyanin, respectively. The two alignments

a. Alignment from crystal structures identity residues:

```
PCY0:5   -AAIVKLGGDDGS-----LAFVPNNITVGAGESIEFINNAGFPHNIVFDEDAVPAGVDVDAIS
PAZ0:24 ENIEVHML---NKGAEGAMVFEPAYIKANPGDTVTFIPVN-KGHNVESIKDMIPEGAEK---F

PCY0: -AXEXDYLNSKGNTVVRKLTTPGTYGVTCDPHSGAGMKMTITVQ
PAZ0: KS----KINE---NYVLTVTNPGAYLVLCTPHYAMGMIALIAVG
```

b. FASTA alignment(short segment):

```
20.4% identity;          Global alignment score: 48 (max)

PCY0: 22 NNITVGAGESIEFINNAGFPHNIVFDEDAVPAGVDVDAISAXEXDYLNSK-YNT
PCY1: 53 AKLTIKPGDTVEFLNNKVPPHNVVFDAALNPAKSADLAKSLSHKQLLMSPGQST
PAZ1: 46 VRL--KPGDSIKFLPT-DKGHNVETIKGMAPDGADYVKTTVGQEAVVKFD---K
PAZ0: 46 IKA--NPGDTVTFIPV-DKGHNVESIKDMIPEGAEKFKSKINENYVLTVT---Q
```

c. FASTA alignment (long segment):

```
30.2% identity;          Global alignment score: 96

PCY0:6  AIV---KLGGDDG-SLAFVPNNITVGAGESIEFINNAGFPHNIVFDEDAVPAGVDVDAISAXEXD
PCY1:37 YTV---KLGSDKG-LLVFEPAKLTIKPGDTVEFLNNKVPPHNVVFDATLNPAKSADLAKSLSHKQ
PAZ1:24 DEVAVKMLNSGPGGMMVFDPALVRLKPGDSIKFL----PTDKGHNVETIK-GMAPDGADYV--K-

PCY0: YLNSKGNTV--VRKLTTP-GTYGVTCDPHSGAGMKMTITVQ
PCY1: LLMSPGQSTSTTFPADAPAGDYSFYCEPHRGAGMVGKITVA
PAZ1: --TTVGQEAVVKF---DKEGVYGFKCAPHYMMGMVA-LVVV
```

FIGURE 1 Sequence alignments of superimposable portions of plastocyanin and pseudoazurin (cupredoxin) template proteins. (*a*) Alignment of plastocyanin (PCY0) from green algae (amino acids 5 through 104) with pseudoazurin from *Alcaligenes faecalis* (amino acids 24 through 116) derived from the x-ray crystal structures of the two proteins (cf. Fig. 2). (*b*) FASTA sequence alignments between plastocyanin from green algae (PCY0 residues 22 to 73) and plastocyanin precursor (PCY 1 residues 53 to 106) with pseudoazurin precursor (PAZ 1 residues 23 to 74) and pseudoazurin (PAZ0 residues 46 to 93). (*c*) FASTA alignment of plastocyanins and pseudoazurin extending over a larger region of the sequence (PCY0 residues 6 to 104), (PCY1 residues 37 to 138), (PAZ1 residues 1 to 97). The identity and global alignment scores are described in the text.

```
PCY0 - sp P07465  pdb 7pcy Plastocyanin - green algae
PCY1 - sp P14114  Plastocyanin precursor
PAZ1 - sp P04171  pdb 1 pmy Pseudoazurin (Cupredoxin) Methylobacterium extorquens
PAZ0 - sp P04377  Pseudoazurin precursor (cupredoxin) Alcaligenes faecalis
Residue 6 on N-terminal of PCY0 (Fig. 2) corresponds to the residue 37 of PCY1 which was used for the FASTA
alignment
```

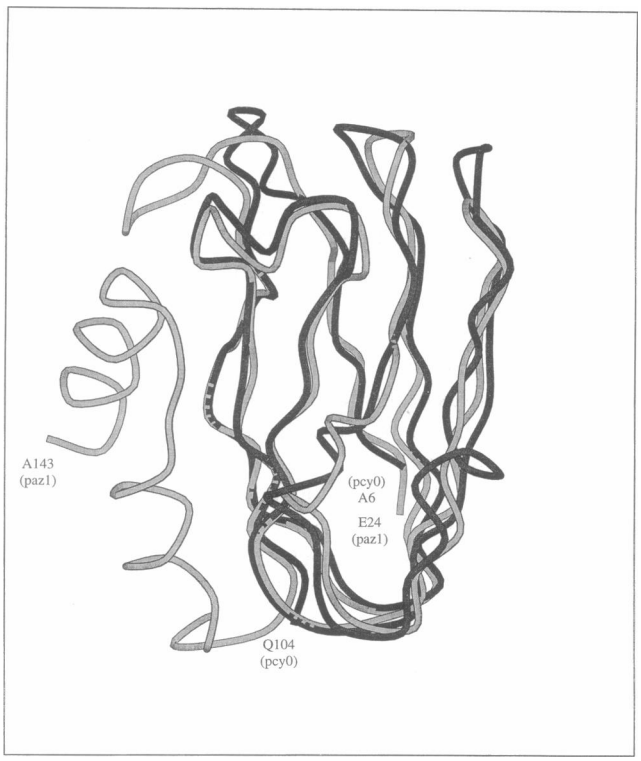

FIGURE 2 Superimposition of the peptide backbone ribbon diagrams of plastocyanin (PCY0) and pseudoazurin (PAZ1). Regions of identity are superimposed for these 105 and 143 amino acid proteins (cf. Guss and Freeman, 1983; Adman et al., 1989). Single letter codes are shown for the positions of amino- and carboxyl-terminal amino acids in the alignment. The picture was created using the MOLSCRIPT program (Kraulis, 1991).

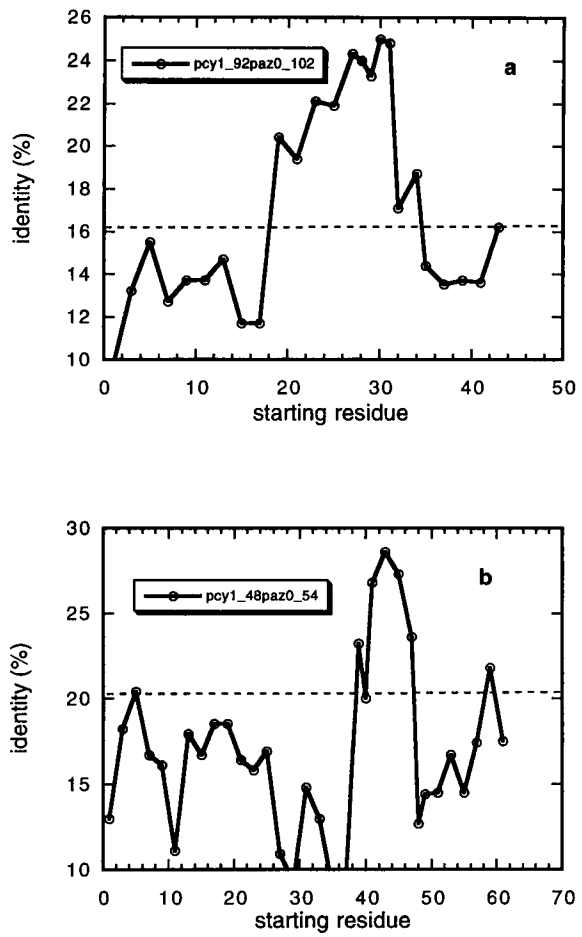

FIGURE 3 FASTA double window analysis of the pseudoazurin and plastocyanin template proteins. (*a*) pseudoazurin (PAZ0) query sequence 92 amino acids starting residue 24; plastocyanin template (PCY1) 102 amino acids. (*b*) PAZ1 query sequence 48 amino acids—starting residue 46; plastocyanin (PCY1) template sequence 55 amino acids. The query sequence was scanned across the template sequence, a single residue at a time as described in Methods. Percent of amino acid identity is plotted for each residue shift and a global alignment score determined for each peak. Details and gap penalties are described in Methods.

reveal a common peak of percent identity between the two proteins; hence, although the two proteins have limited sequence identity, the double window FASTA alignment correctly identifies sequences that superimpose in the tertiary structures.

Sequence alignments between copper binding and nAChR families of proteins

Several representatives of the nAChR superfamily of subunits showed sequence similarity with the family of copper binding proteins when analyzed using the FASTA double window alignment. Fig. 4, *a–c* shows the double window identity scores from alignment of pseudoazurin 1 and plastocyanin 1 versus extracellular domains of the α_1-, α_3-, and α_4-subunits of nAChR. A maximum sequence identity and global alignment score appear with the starting amino acid residue 55 of the α_1-subunit template (windows of 54 amino acids for α_1 versus 48 amino acids of pseudoazurin 1). The global alignment score is calculated by FASTA using the matrix that weights amino acid substitutions and also accords higher penalty scores for the first residue in a gap and smaller penalty scores for the rest of the residues in a gap (Pearson, 1990, 1996). We used a *codaa* matrix where the value of the substitution penalty is weighted by the probability of genetic mutation. The sequence of pseudoazurin shows an identity of 32.7% with the sequence of the α-subunit extracellular domain. Maxima in identical positions also exist for α_3- and α_4-subunits (Fig. 4, *b* and *c*), although the homology scores are not as high. Different residue gap selections give rise to the multiple peaks.

When the query window of 55 residues of plastocyanin was used versus the same family of the nAChR α-subunits (Fig. 4, *d–f*), the maximum for correspondence of amino acid identity and highest global alignment scores of *codaa* matrix were found starting with residue 65 of the template window for all α-subunits.

A well-defined maximum of amino acid identity was found for the α_1-subunit of the nAChR with pseudoazurin using the larger windows (102 residues of α_1-subunit versus 92 residue of pseudoazurin-1) (Fig. 4 *g*). The alignment using the larger windows corresponds in amino acid posi-

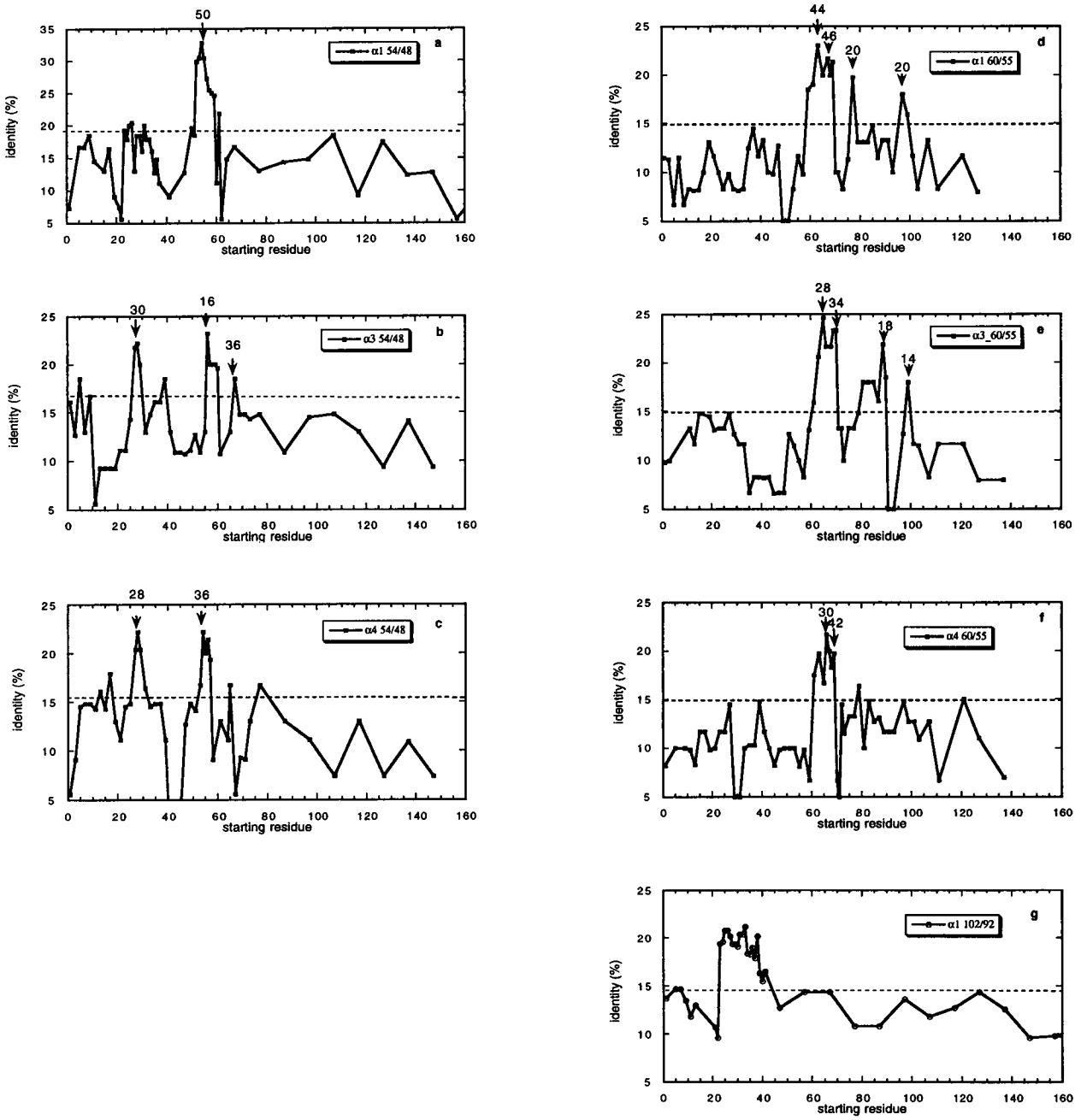

FIGURE 4 FASTA double window screen for α-subunits of nAChR, and copper binding proteins pseudoazurin (PAZ1) and plastocyanin (PCY1). The 48 amino acid sequence window of PAZ1 used is:

VRLKPGDSIKFLPTDKGHNVETIKGMAPDGADYVKTTVGQEAVVKFDK;

the 55 amino acid sequence window of PCY1 used is:

KPGDTVEFLNNKVPPHNVVFDATLNPAKSADLAKSLSHKQLLMSPGQSTSTTFPA;

(*a*) nAChR-α_1 54 amino acids vs PAZ1; (*b*) nAChR-α_3 54 amino acids vs PAZ1; (*c*) nAChR-α_4 54 amino acids vs PAZ1; (*d*) nAChR-α_1 60 amino acids vs PCY1; (*e*) nAChR-α_3 60 amino acids vs PCY1; (*f*) nAChR-α_4 60 amino acids vs PCY1. (*g*) nAChR-α_1 102 amino acids vs PAZ1 92 amino acids extending from residue 1.

tion to the alignment using smaller windows (54 nAChR versus 48 pseudoazurin) shown in Fig. 4 *a*.

Alignments corresponding to the respective maxima on double window plots are shown in Fig. 5. Sequence similarity occurs in the corresponding homologous regions of α_1-, α_3-, and α_4-subunits. Maxima in the same region were also found for the double window alignment of plastocyanin versus $GABA_A$ and $GABA_B$ receptor extracellular domains

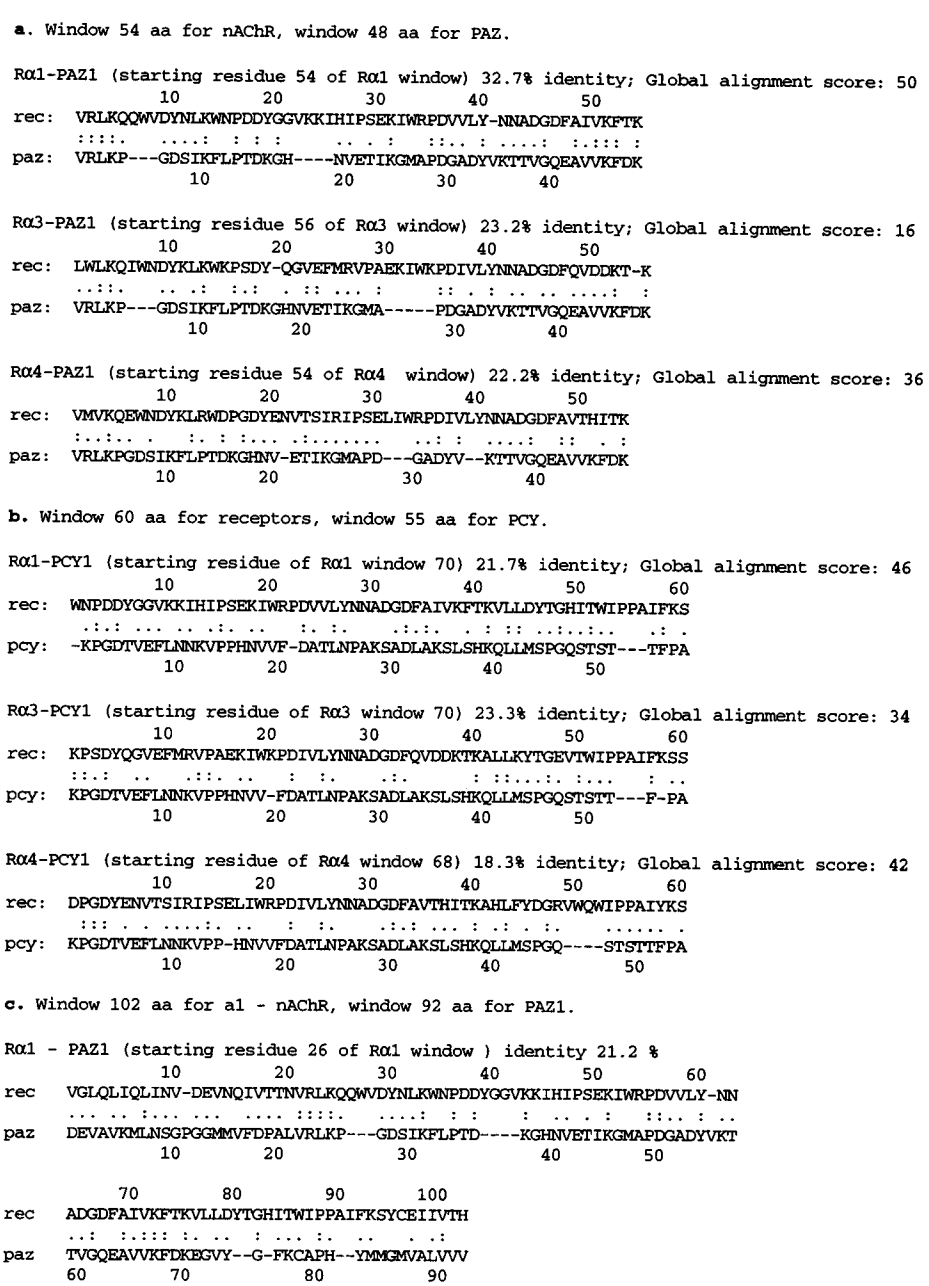

FIGURE 5 Correspondences between the aligned sequences of the extracellular domain of α-subunits of the nAChR and copper binding proteins: (*a*) nAChRα_1 window 54 vs PAZ1 window 48 aa; (*b*) nAChR α_1, α_3, and α_4 with window containing 60 amino acids starting from the residues 60, 70, and 68, respectively, vs PCY window 55 aa. (*c*) nAChRα_1 window 102 to PAZ 92 aa. Scoring matrix: *codaa.mat*, gap penalties: $-12/-4$

(data not shown). Maxima for β_1-, γ, α_7-, and δ-subunits of the nAChR were far smaller and bordered on the 20% level of significance.

The preceding results support the hypothesis that the sequence similarity shared by the pseudoazurins and plastocyanins is applicable to the superfamily of nAChR subunits. The α_7- and γ- and δ-subunits diverged from the other α-subunits early in evolution (Novere and Changeux, 1995), and the early divergence may account for the diminished sequence identity seen for these subunits in the FASTA alignments.

Fig. 6 shows the tabulation of the multiple sequences for four of the nAChR subunits (α_1, β_1, γ, and δ), and the five copper binding proteins (pseudoazurin, pseudoazurin (precursor), auracyanin, rusticyanin, and plastocyanin 1). The individual pairwise alignments, which extended to 32.7% for 48 overlapping amino acids, were subsequently adjusted to achieve the best fit in the multiple family alignment. Percentage identity between family representatives was 42.1% between residues 62 and 162 in the receptor subunits. (Identity in this multiple alignment was scored as 1 when one of the amino acids from the copper binding protein family was identical with one of the amino acids of the receptor family, and as 0 when no such identity was found.) The overall regions extend from residues 29 to 164 in the α-subunit of the nAChR, from residue 14 to 106 in plastocyanin, and from residue 34 to residue 143 in pseudoazurin 1. The bold lettering shows residues of identity between the

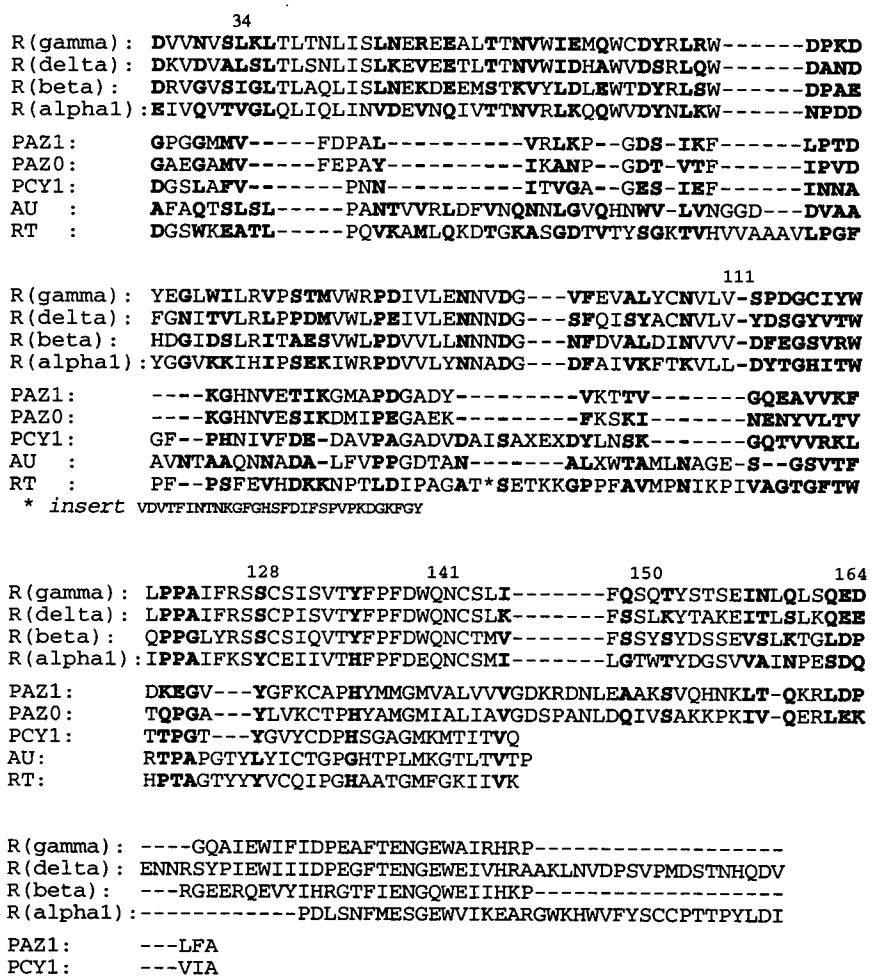

FIGURE 6 Multiple sequence alignments for the muscle nicotinic acetylcholine receptor subunits α, β, γ, and δ, and pseudoazurin (PAZ1), pseudoazurin precursor (PAZ0), auracyanin (Au), rusticyanin (RT), and plastocyanin (PC). The numbering on the top corresponds to the α_1-subunit of the nAChR. The overall alignment is based on the corresponding pair alignments. The residues in bold indicate sequence identities between two members of the respective families.

two families of proteins. Our investigations of possible alignments of the lysine-, arginine-, and ornithine-binding protein (LAOBP) and the excitatory amino acid receptors (Stern-Bach et al., 1994; Wo and Oswald, 1994; Sutcliffe et al., 1996) with the nAChR subunits did not yield strong similarities in sequence, as noted previously by Cockroft et al., (1990) when comparing nAChR with the kainate binding proteins.

Surprisingly, the family of copper binding proteins show rather limited amino acid identity within their members (Fig. 6). The closest relatives of this family, pseudoazurin and pseudoazurin precursor, have 45% identity in a common domain of 120 amino acids. Analysis of difference matrices shows the sequences diverge >90% for the pairs in this family (Ryden and Hunt, 1993).

The copper binding proteins function in electron transfer and show some structural identity with the higher molecular-weight copper transport proteins such as ceruloplasmin (Messerschmidt and Huber, 1990; Ryden and Hunt, 1993). The copper binding proteins are thought to be early arrivals on an evolutionary time scale with their presence in prokaryotes, plants, and animals; in fact, plastocyanin and azurin diverged during the period when cyanobacteria separated from eubacteria, perhaps as much as three billion years ago (Ryden and Hunt, 1993). As such they may be common distant ancestors for several families of proteins, including the nAChR.

Structural model of the extracellular domain of nAChR subunits

The model of folding of the nAChR subunits was constructed according to the tertiary structures of the template proteins, with nontemplate segments inserted and oriented according to residue disposition predicted by site-specific labeling and mutagenesis studies, as described in Methods. The region modeled on the basis of the copper binding template proteins extends from residues 39 through 164 of the nAChR α-subunit; regions amino- and carboxyl-terminal to this segment fall outside the region of the template proteins. Fig. 7 shows homologous portions of pseudoazurin and nAChR α-subunit superimposed. Four insertions in the α_1-subunit were included: 1) a loop between residues 85 and 96 oriented to the (+) face according to labeling of αY93, 2) a loop between residues 104 and 111 oriented to the (−) face according to the conotoxin M1 determinant γS111/δY113, 3) a loop between residues 67 and 76 ori-

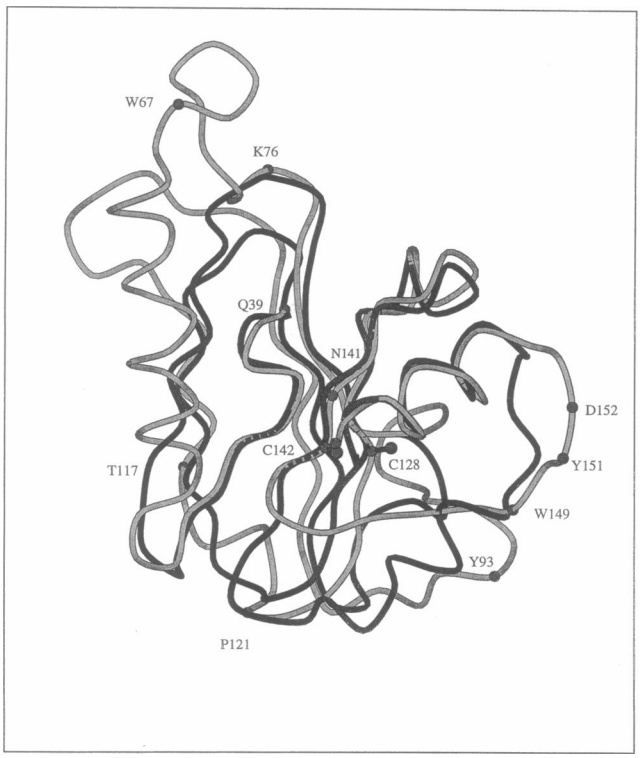

FIGURE 7 Superimposition of ribbon diagrams of pseudoazurin (PAZ1) (*black*) and the α-subunit of nicotinic acetylcholine receptor (*gray*). Shown are the α-carbon backbone of PAZ1 from the x-ray crystallographic structure (Adman et al., 1989) from residues 41 to 143 and the modeled structure of the α-subunit of the nAChR from the residues 39 to 164. Specific residues in the nAChR α-subunit are denoted by the black rings. The Cα and Cβ atoms are only shown for C128 and C142. The clockwise or (−) face is shown by the helix on the left, and the counterclockwise or (+) face by Y93, W149, Y151, and D152 on the right. The picture was created using the MOLSCRIPT program (Kraulis, 1991).

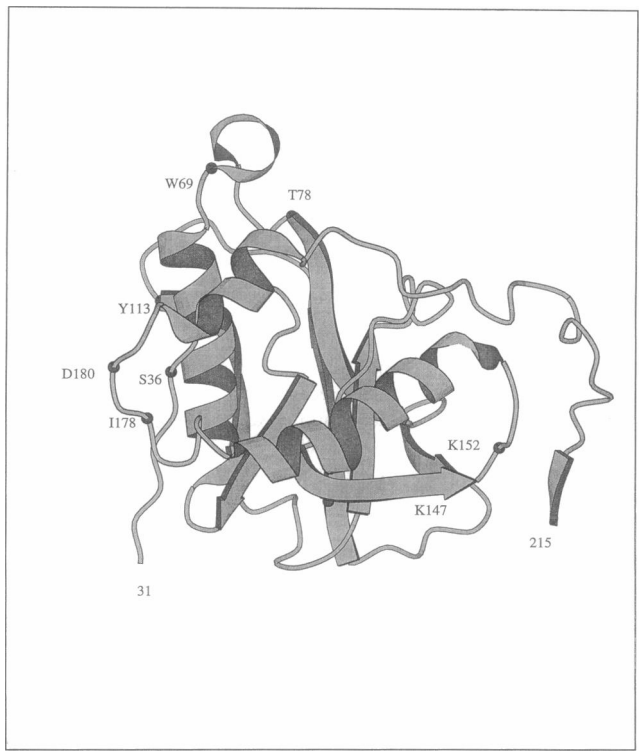

FIGURE 8 Ribbon diagram of the δ-subunit of nAChR between residues 31 and 214. The model was developed from the sequence homology between residues 39 and 164 identified in Fig. 6 and residue locations detailed in Table 1. The counterclockwise or (−) face and the clockwise or (+) face lie on the left and right of the figure. The picture was created using the MOLSCRIPT program (Kraulis, 1991).

ented to the synaptic extreme of the subunit according to binding of mAb35, and 4) the region between residues 48 and 63. The Chou-Fasman algorithm predicts the latter region to be a helical structure so residues 48 through 63 are modeled as a helix rather than the extended structure in the template proteins. These residues are positioned on the (−) face by virtue of labeling studies of γW55 and mutagenesis of γE57.

Fig. 8 shows the model of the homologous nAChR δ-subunit. It includes a carboxyl-terminal extension from the template protein, a helix extending from the (+) to the (−) face, an extended structure at the (−) face harboring γF172/δI178 assigned from α-conotoxin binding, and a helix followed by a β strand extending back to the (+) face, which in the α_1-subunit harbors αY190, αC192/C193, and αY198. All these residues have been shown to be critical for ligand binding. Thus the model of the nAChR subunits contains three helices, between residues 48 and 63, 153 and 163, and 180 and 185, with the remaining structure containing nine β strands.

Projection and three-dimensional maps of the *Torpedo* receptor obtained from electron microscopy show one dominant and two less evident rodlike densities that are oriented approximately normal to the membrane (Unwin, 1993; 1996). The rods are suggestive of an α-helix structure. The ligand binding site was proposed to be encircled by the three rods placing it near the transverse center of the α-subunit but above the plane of the membrane (Unwin, 1993; 1996). The dominant rod may correspond to the 48 to 63 helix, but the two shorter helices in our model are not normal to the membrane (cf. Fig. 8). However, the tilts of the helix may differ in the individual subunits and are influenced by bound ligand (Unwin, 1995). A helix may also exist in the first 30 residues for which we lack the structural information. Our placement of the binding site at the subunit interface, which is based on the identification of the involved residues and the homology modeling, differs from the proposed location in the electron microscopy reconstruction.

Disulfide loop

The disulfide loop common to all nicotinic receptors and other members of this receptor family is located between the Cys-128 and Cys-142 (α-subunit numbering).The position of the loop will constrain the interior β strands in the region contributing to a flat surface. The position of these two Cys

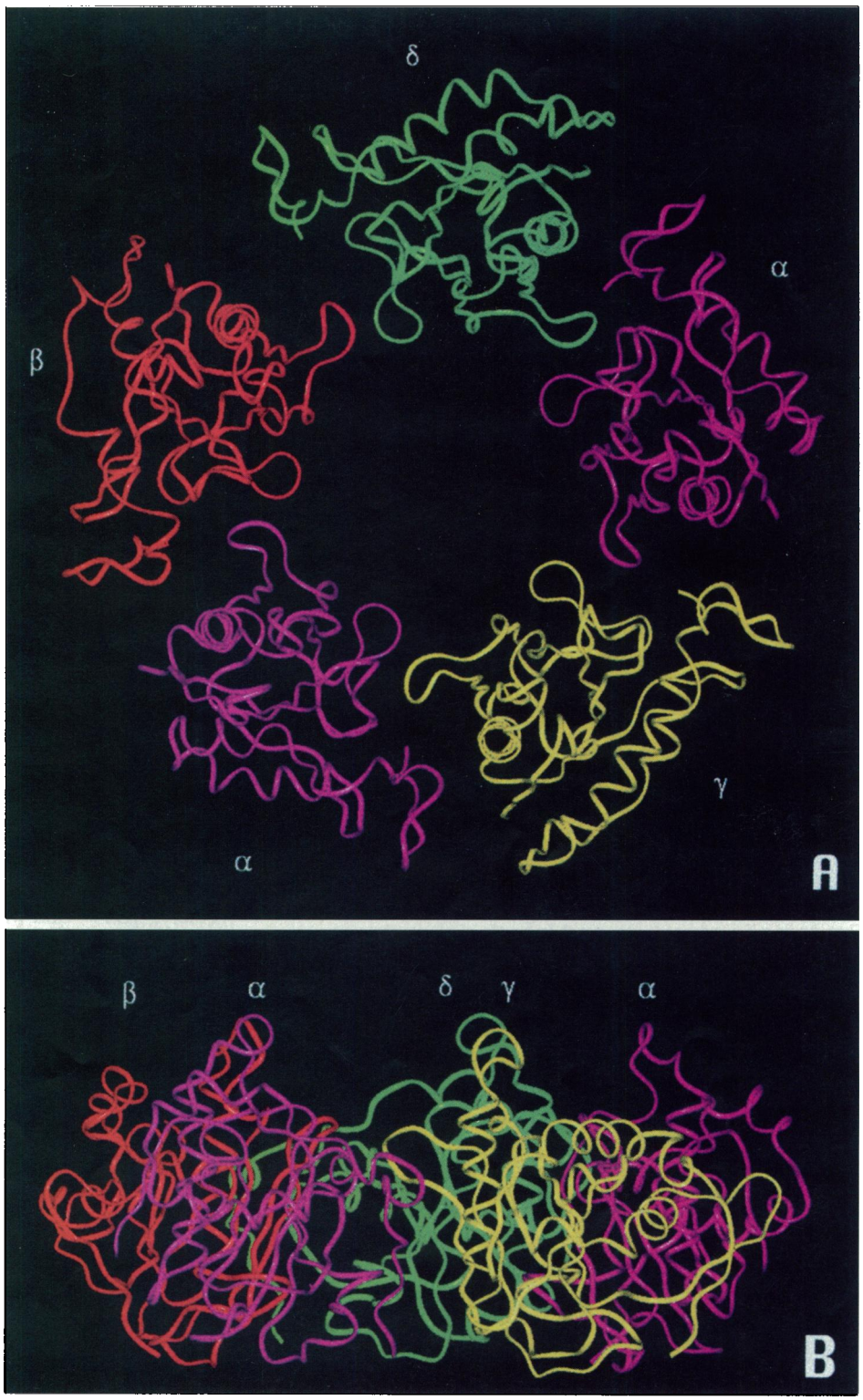

FIGURE 9 Ribbon diagram of the extracellular domain of the pentameric nAChR. (*A*) Top view, (*B*) side view. See text for procedures used in modeling.

in the nAChR appears symmetrical around the triad Thr-133, Tyr or His-134, and Phe-135 at the tip of the loop. In pseudoazurin, the structural loop also shows a single turn around the triad Phe-133, His-134, and Tyr-135. Pseudoazurin contains only one Cys residue, which may not necessarily superimpose on either Cys-128 or Cys-142.

Glycosylation site

Asn-141, a glycosylation site in the extracellular domain of nAChR, is sufficiently solvent-accessible in the model to support a surface oligosaccharide. Upon mutation to form a glycosylation consensus signal, glycosylation also occurs at

residues 152 (Sugiyama et al., 1996), 187, and 189 (Keller et al., 1995); these residues also show potential solvent accessibility.

Possible membrane contact surfaces

Two regions in the nAChR extracellular domain are likely to come in close apposition to the extracellular membrane face; they contain the following sets of hydrophobic residues: Val-46, Thr-49 and Leu-119, Pro-121, Ile-123, and Phe-124. The model also places two negatively charged residues that may come into close proximity to the membrane: Glu-48 and Asp-97. Proximity of positively charged residues αLys-125, γArg-125, and α and γArg-87 would confer electrostatic neutrality to the overall "membrane face" of the nAChR subunits.

Main immunogenic region

The main immunogenic region that encompasses residues 67–76 (Tzartos et al., 1988) in the nAChR was shown to be located at the extreme synaptic apex of the α-subunits (Beroukhim and Unwin, 1995). Moreover, the location of the antibody binding site is shown to be near the interface between each α and its neighboring subunit. In the model the region between residues 67 and 76 is the domain furthest from the membrane in each subunit; it contains a turn that completes the end of α-helix 1 (residue 65) of each subunit.

Pentameric structure and interfacial surfaces

Each subunit in its possible folded conformation was positioned on the membrane surface using the following considerations: 1) a position of the main immunogenic region distal to the membrane; 2) a pentameric arrangement of subunits abutting but not occluding an internal pore; 3) dimensions consistent with the overall size of the receptor: extracellular domain ~65 Å in length, a maximum diameter of ~80–85 Å, and a pore opening of 20–25 Å (Unwin, 1993, 1996); 4) experimental results positioning particular residues at the (+) and (−) subunit interfaces; and 5) pseudosymmetry around a central pore.

The subunits were then docked to minimize electrostatic repulsion. The model (Fig. 9) has the following geometrical dimensions: the height of the extracellular domain ~56 Å, the external diameter of the pentamer ~90 Å, the diameter of the pore vestibule ~24 Å.

Ligand binding sites

Figure 10 shows the apposition of the α- and γ-subunits to form the ligand binding site. We chose two ligands to illustrate residues in the two subunits that contribute to the binding site, *d*-tubocurarine and α-conotoxin M1. Based on its crystal structure (Codding and James, 1973), the rigid *d*-tubocurarine molecule can be docked between Y117 of the γ-subunit and Y198 of the α-subunit. In the model, the two tyrosines are separated by 10 Å, a distance which would allow them to stabilize the two quaternary ammonium groups in *d*-tubocurarine (Fu and Sine, 1994).

α-Conotoxin M1 is a 14-amino acid peptide that forms a rigid triangular structure owing to its internal disulfide bridges (Myers et al., 1991). Two of the three points of the triangle contain positive charges, the amino-terminal nitrogen and arginine at position 10 (Guddat et al., 1996), perhaps allowing it to bridge the subunit interface analogously to *d*-tubocurarine. Although points of contact in the nAChR have not been identified, the model places residues contributing to α-conotoxin M1 binding at appropriate (+) or (−) face. The pair of interacting residues, γK34 and γF172, are positioned at the (−) face of the subunit, and are close enough to each other to form an interdependent contribution to conotoxin M1 affinity (Sine et al., 1995). Similarly, γS111 is positioned at the (−) face for interaction with conotoxin M1. On the other hand, residues α93, α152, and the segment between residues 180 and 200 are correctly positioned at the (+) face for interaction with α-conotoxin M1.

The model also places other residues that contribute to ligand affinity to the (+) or (−) face predicted by chemical labeling or mutagenesis. The aromatic residues αY93, αW149, αY151, αY190, and αY198 are located on the (+) face and are seen to form an aromatic pathway leading from the perimeter to the interior of the subunit interface. Conversely, γD174 and γE55 are located at the (−) face.

Based on competition (Table 1) and cross-linking studies (Oswald and Changeux, 1982), the 6.5–7.5 kDa α-neurotoxins are expected to bind at the αγ and αδ interfaces, and the tips of the loops of the three fingered α-neurotoxins appear critical for interaction (Tremeau et al., 1995). Future thermodynamic mutant cycle analyses may enable one to describe the likely orientation of these larger peptides at the two subunit interfaces.

Electrostatic properties of the extracellular domain

The highly negative electrostatic potential of the extracellular domains of the nAChR subunits (−55 e for the pentamer) limits the orientations in which they are likely to form inter-subunit contacts. In our model, the interfaces of subunits are dominated by uncharged, hydrophobic residues. A disposition of amino acid residues where the contact surfaces of opposing subunits contain hydrophobic residues is consistent with the pentameric ring structure of the receptor (Unwin, 1993) and with the observation that the residues in the extracellular region dictate the specificity of subunit assembly (Kreienkamp et al., 1995).

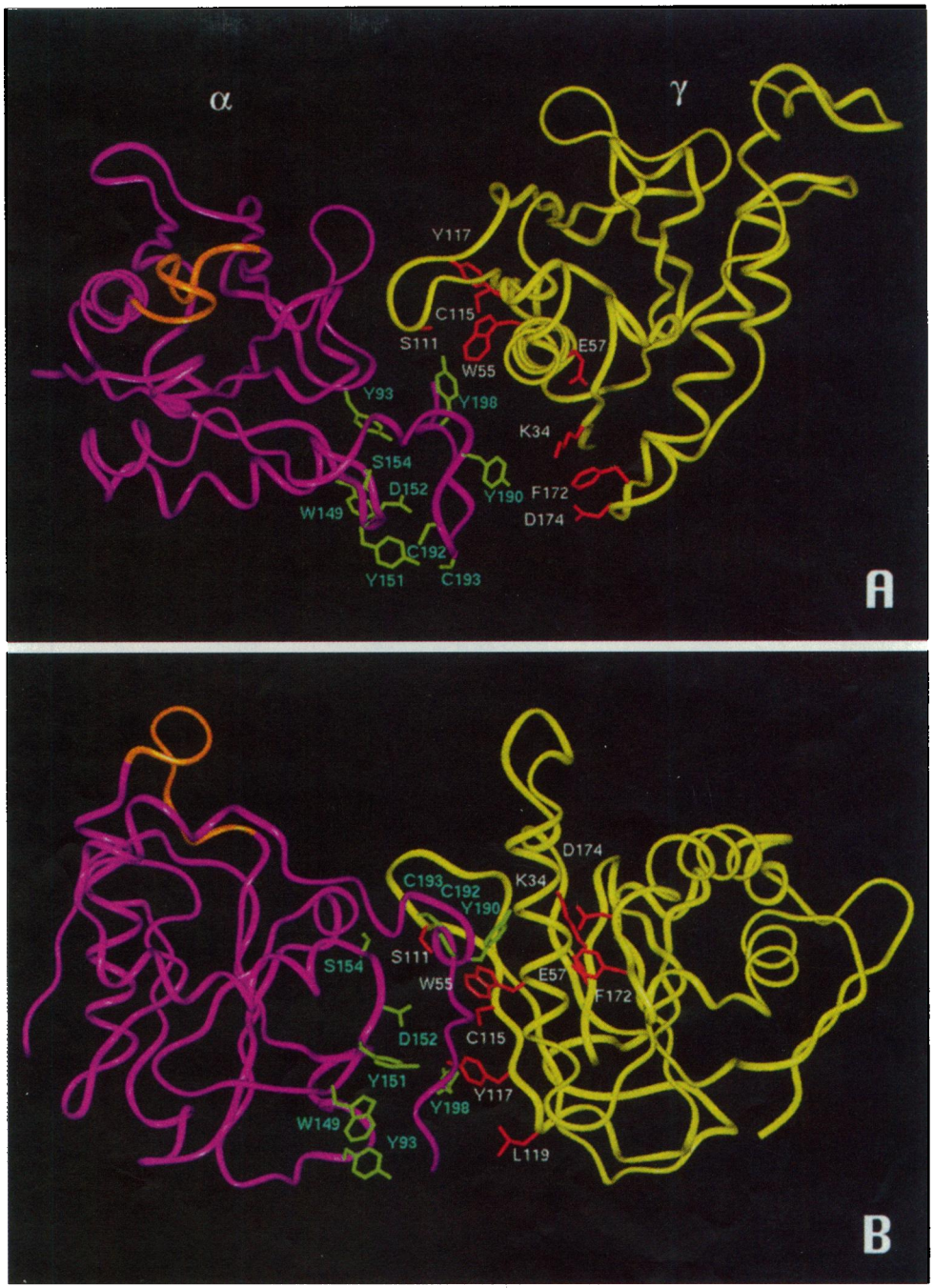

FIGURE 10 Ribbon diagram of the α- and γ-subunits enlarged from Fig. 9: (*A*) top view, (*B*) side view. The side chains of residues identified to be important in ligand binding (see Table 1) at this interface are shown in stick representations: α-subunit: Y93, W149, Y151, D152, S154, Y190, C192, C193, and Y198; γ-subunit: K34, W55, E57, S111, C115, Y117, F172, and D174. The main immunogenic region (residues 67–76) in the α-subunit is shown in *orange*.

Electrostatic field differences at the α-γ, α-δ interfaces

Figure 11 shows the electrostatic potential of the receptor at ±1.0 e (red, negative; blue, positive; white, zero potential). From a more distal position of the ligand, the nAChR shows a negative surface, but the interfacial region between β and δ has electrostatically neutral regions and should not attract a positive ligand. Moreover, of the five subunit interfaces δβ, βα and, to a lesser extent, γα, present mostly stable non-negative potential surfaces to the positive ligand at any precollisional distance. By contrast, the αγ, and to lesser extent αδ, interfaces present mostly negative potential surfaces. Thus, electrostatic considerations in this assembled model of subunits show surface charge characteristics consistent with preferential association of cationic ligands with the αγ and αδ interfaces.

Limitations of the model

The paucity of data on the structure of certain regions of the nAChR requires that several caveats be mentioned for the working model presented here. First, we are without structural information on the amino-terminal 30 amino acids, the loop between transmembrane domains 2 and 3 (residues 281

FIGURE 11 Equipotential surfaces of nAChR. Top view of nAChR. Potential ±1 kT/e. *Red*, negative potential, *white*, zero potential, *blue*, positive potential.

to 286), and the extracellular carboxyl-terminus of approximately nine residues. How these regions interact with the domains that have been modeled is not known. The region from amino acid 164 to the beginning of transmembrane domain M1 (residue 210) is not homologous with the copper binding protein family, and residue positions are derived only from ligand binding, solvent exposure, and subunit association data. Copper binding proteins also lack a disulfide bond corresponding to Cys-128 and Cys-142, yet a general loop placing these residues in proximity is evident. Our treatment also cannot exclude the possibility that portions of the extracellular domain associate with the membrane surface or that a hydrophobic loop dips into membrane.

Those regions showing sequence identity to the copper binding proteins and allowing positioning of side chains from chemical and mutagenesis data provide the nucleus for the development of the structural template. As further data emerge, modifications and additions should be entertained. The attractive features of the model lie in the consistency of placement of residues identified in labeling and mutagenesis experiments. Finally, the model distinguishes on the basis of electrostatics the two ligand binding interfaces from the other three where ligand binding is believed to be absent.

The authors thank Drs. Russell Doolittle and Christopher Wills (University of California, San Diego) for valued discussions and suggestions regarding the alignment procedures.

This research was supported by United States Public Health Service Grants GM 18360 (to P.T.) and NS 31744 (to S.M.S.).

REFERENCES

Abramson, S. N., Y. Li, P. Culver, and P. Taylor. 1989. An analog of lophotoxin reacts covalently with tyrosine 190 in the α-subunit of the nicotinic acetylcholine receptor. *J. Biol. Chem.* 264:12666–12672.

Adman, E. T., S. Turley, R. Bramson, K. Petratos, D. Banner, D. Tsernoglou, T. Beppu, and H. Watanabe. 1989. A 2.0-A structure of the blue copper protein (cupredoxin) from Alcaligenes faecalis S-6. *J. Biol. Chem.* 264:87–99.

Aylwin, M. L., and M. M. White. 1994. Gating properties of mutant acetylcholine receptors. *Mol. Pharmacol.* 46:1149–1155.

Beroukhim, R., and N. Unwin. 1995. Three-dimensional location of the main immunogenic region of the acetylcholine receptor. *Neuron.* 15: 323–331.

Blount, P., and J. P. Merlie. 1989. Molecular basis for the two nonequivalent ligand binding sites of the muscle nicotinic acetylcholine receptor. *Neuron.* 3:349–357.

Changeux, J.-P. 1995. The acetylcholine receptor: a model for allosteric membrane proteins. *Biochem. Soc. Trans.* 23:195–205.

Chiara, D. C., and J. B. Cohen. 1992. Identification of amino acids contributing to high and low affinity *d*-tubocurarine (*d*TC) sites on the *Torpedo* nicotinic acetylcholine receptor (nAChR) subunits. *Biophys. J.* 61:A106.

Cockroft, V. B., G. G. Lunt, and D. J. Osguthorpe. 1990. Modeling of binding sites of nicotinic acetylcholine receptor and their relation to models of the whole receptor. *Biochem. Soc. Symp.* 57:65–79.

Codding, P. W., and M. N. G. James. 1973. The crystal and molecular structure of a potent neuromuscular blocking agent: *d*-tubocurarine dichloride pentahydrate. *Acta Crystallogr. B.* 29:935–942.

Cohen, J. B., S. D. Sharp, and W. S. Liu. 1991. Structure of the agonist-binding site of the nicotinic acetylcholine receptor, *J. Biol. Chem.* 266: 23354–23364.

Corringer, P. J., J.-L. Galzi, J.-L. Eisele, S. Bertrand, J.-P. Changeux, and D. Bertrand. 1995. Identification of a new component of the agonist site of the nicotinic α7 homooligomeric receptor. *J. Biol. Chem.* 27: 11749–11752.

Czajkowski, C., and A. Karlin. 1991. Agonist binding site of *Torpedo* electric tissue nicotinic acetylcholine receptor. *J. Biol. Chem.* 266: 22603–22612.

Czajkowski, C., and A. Karlin. 1995. Structure of the nicotinic receptor acetylcholine-binding site. *J. Biol. Chem.* 1995:3160–3164.

Czajkowski, C., C. Kaufmann, and A. Karlin. 1993. Negatively charged amino acid residues in the nicotinic receptor δ subunit that contribute to the binding of acetylcholine. *Proc. Natl. Acad. Sci. USA.* 90:6285–6289.

Dennis, M., J. Giraudat, F. Kotzyba-Hibert, M. Goeldner, C. Hirth, J.-Y. Chang, C. Lazure, M. Chretien, and J.-P. Changeux. 1988. Amino acids of the *Torpedo marmorata* acetylcholine receptor α-subunit labeled by a photoaffinity ligand for the acetylcholine receptor by photoaffinity labeling. *J. Biol. Chem.* 265:10430–10437.

Doolittle, R. F. 1990. Searching through sequence databases. *Methods Enzymol.* 187:99–110.

Fitch, W. M. 1966. An improved method of testing for evolutionary homology. *J. Mol. Biol.* 16:9–16.

Fu, D.-X., and S. M. Sine. 1994. Competitive antagonists bridge the α-γ subunit interface of the acetylcholine receptor through quaternary ammonium-aromatic interactions. *J. Biol. Chem.* 269:26152–26157.

Galzi, J.-L., F. Revah, D. Black, M. Goeldner, C. Hirth, and J.-P. Changeux. 1990. Identification of a novel amino acid α-tyrosine 93 within the cholinergic ligands-binding sites of the acetylcholine receptor by photoaffinity labeling. *J. Biol. Chem.* 265:10430–10437.

Gilson, M., and B. Honig. 1988. Calculations of electrostatic potentials in an enzyme active site. *Proteins.* 4:7–18.

Gu, Y., J. Forsayeth, S. Verall, X. Yu, and Z. Hall. 1991. Assembly of the mammalian muscle acetylcholine receptor in transfected COS cells. *J. Cell. Chem.* 114:779–807.

Guddat, L. W., J. A. Martin, L. Shan, A. B. Edmundson, and W. R. Gray. 1996. Three-dimensional structure of α-conotoxin G1 at 1.2 Å resolution. *Biochemistry.* 35:11329–11335.

Guss, J. M., and H. C. Freeman. 1983. Structure of oxidized poplar plastocyanin at 1.6 Å resolution. *J. Mol. Biol.* 169:521–563.

Hultner, M., D. W. Smith, and C. Wills. 1994. Similarity landscapes: a way to detect many structural and sequence motifs in both introns and exons. *J. Mol. Evol.* 38:188–203.

Kao, P. N., A. J. Dwork, R. J. Kaldany, M. L. Silver, J. Wideman, S. Stein, and A. Karlin. 1984. Identification of the α subunit half-cystine specifically labeled by an affinity reagent for the acetylcholine receptor binding site. *J. Biol. Chem.* 259:11662–11665.

Karlin, A., and M. H. Akabas. 1995. Towards a structural basis for the function of nicotinic acetylcholine receptors and their cousins. *Neuron.* 15:1231–1244.

Keller, S. H., H.-J. Kreienkamp. C. Kawanishi, and P. Taylor. 1995. Molecular determinants conferring alpha toxin resistance in recombinant DNA-derived acetylcholine receptors. *J. Biol. Chem.* 270:4165–4171.

Kraulis, P. J. 1991. MOLSCRIPT: a program to produce both detailed and schematic plots of protein structures. *J. Appl. Crystallogr.* 24:946–950.

Kreienkamp, H.-J., R. K. Maeda, S. M. Sine, and P. Taylor. 1995. Intersubunit contacts governing assembly of the mammalian nicotinic acetylcholine receptor. *Neuron.* 14: 635–644.

Machold, J., C. Weise, Y. Utkin, V. Tsetlin, and F. Hucho. 1995. The handedness of the subunit arrangement of the nicotinic acetylcholine receptor from *Torpedo californica. Eur. J. Biochem.* 234:427–430.

Messerschmidt, A., and R. Huber. 1990. The blue oxidases, ascorbate oxidase, laccase and ceruloplasmin. Modeling and structural relationships. *Eur. J. Biochem.* 187:341–352.

Middleton, R. E., and J. B. Cohen. 1991. Mapping of the acetylcholine binding site of the nicotinic acetylcholine receptor: [3H]nicotine as an agonist photoaffinity label. *Biochemistry.* 30:6987–6997.

Myers, R. A., G. C. Zafaralla, W. R. Gray, J. Abbott, L. J. Cruz, and B. M. Olivera. 1991. α-Conotoxins, small peptide probes of nicotinic acetylcholine receptors. *Biochemistry.* 30:9370–9377.

Novere, N. L., and J.-P. Changeux. 1995. Molecular evolution of the nicotinic acetylcholine receptor: an example of multigene family in excitable cells. *J. Mol. Evol.* 40:155–172.

Nowak, M. W., P. C. Kearney, J. R. Sampson, M. E. Saks, C. G. Labarca, S. K. Silverman, W. Zhong, J. Thorson, J. N. Abelson, N. Davidson, P. G. Schultz, D. A. Dougherty, and H. A. Lester. 1995. Nicotinic receptor binding site probed with unnatural amino acid incorporation in intact cells. *Science.* 268:439–442.

Nunzi, F., M. Woudstra, D. Campese, J. Bonicell, D. Morin, and M. Bruschi. 1993. Amino-acid sequence of rusticyanin from *Thiobacillus ferrooxidans*, and its comparison with other blue copper proteins. *Biochim. Biophys. Acta.* 1162:28–34.

O'Hara, P., P. O. Sheppard, H. Thorgersen, D. Venezia, B. A. Haldeman, V. McGrane, K. H. Houamed, C. Thomsen, T. C. Gilbert, and E. R. Mulvihill. 1993. The ligand binding domain in metabotropic glutamate receptors is related to bacterial periplasmic binding proteins. *Neuron.* 11:41–52.

Ohno, K., H. L. Wang, M. Milone, N. Bren, J. Brengman, S. Nakano, P. Quiram, J. Pruitt, S. M. Sine, and A. Engel. 1996. Congenital myasthenic syndrome caused by decreased agonist binding affinity due to mutation in acetylcholine receptor ε-subunit. *Neuron.* 17:157–170.

O'Leary, M. E., and M. M. White. 1992. Mutational analysis of ligand-induced activation of the *Torpedo* acetylcholine receptor. *J. Biol. Chem.* 267:8360–8365.

O'Leary, M. E., G. N. Filatov, and M. M. White. 1994. Characterization of the *d*-tubocurarine binding site of *Torpedo* acetylcholine receptor. *Am. J. Physiol.* 266:C948–C653.

Oswald, R. E., and J.-P. Changeux. 1982. Cross-linking of a-bungarotoxin to the acetylcholine receptor from *Torpedo marmorata* by ultraviolet light irradiation. *FEBS Lett.* 139:225–229.

Pearson, W. R. 1990. Rapid and sensitive sequence comparison with FASTP and FASTA. *Methods Enzymol.* 183:63–98.

Pearson, W. R. 1996. Effective protein sequence comparison. *Methods Enzymol.* 266:227–258.

Pearson, W. R., and D. J. Lipman. 1988. Improved tools for biological sequence comparison. *Proc. Natl. Acad. Sci. USA.* 85:2444–2448.

Prince, R. J., and S. M. Sine. 1996. Molecular dissection of subunit interfaces in the acetylcholine receptor: identification of residues that determine agonist selectivity. *J. Biol. Chem.* 42:25770–25777.

Ryden, L. G., and L. T. Hunt. 1993. Evolution of protein complexity: the blue copper-containing oxidases and related proteins. *J. Mol. Evol.* 36: 41–66.

Sine, S. M. 1993. Molecular dissection of subunit interfaces in the acetylcholine receptor: identification of residues that determine curare selectivity. *Proc. Natl. Acad. Sci. USA.* 90:9436–9440.

Sine, S. M., and T. Claudio. 1991. Gamma- and delta-subunits regulate the affinity and the cooperativity of ligand binding to the acetylcholine receptor. *J. Biol. Chem.* 266:19369–19377.

Sine, S. M., H.-J. Kreienkamp, N. Bren, R. Maeda, and P. Taylor. 1995. Molecular dissection of subunit interfaces in the acetylcholine receptor: identification of determinants of α-conotoxin M1 selectivity. *Neuron.* 15:205–211.

Sine, S. M., P. Quiram, F. Papanicolau, H.-J. Kreienkamp, and P. Taylor. 1994. Conserved tyrosines in the α subunit of the nicotinic acetylcholine receptor stabilize quarternary ammonium groups of agonists and curariform antagonists. *J. Biol. Chem.* 269:8808–8816.

Stern-Bach, Y., B. Bettler, M. Hartley, P. O. Sheppard, P. J. O'Hara, and S. F. Heinemann. 1994. Agonist selectivity of the glutamate receptor specified by two domains structurally related to bacterial amino acid-binding proteins. *Neuron.* 13:1345–1357.

Sugiyama, N., A. E. Boyd, and P. Taylor. 1996. Anionic residue in the α-subunit of the nicotinic acetylcholine receptor contributing to subunit assembly and ligand binding. *J. Biol. Chem.* 271:26575–26581.

Sutcliffe, M. J., Z. G. Wo, and R. E. Oswald. 1996. Three-dimensional models of non-NMDA glutamate receptors. *Biophys. J.* 70:1575–1589.

Tomaselli, G. F., J. T. McLaughlin, M. E. Jurman, E. Hawrot, and G. Yellen. 1991. Mutations affecting agonist sensitivity of the nicotinic acetylcholine receptor. *Biophys. J.* 60:721–727.

Tremeau, O., C. Lemaire, P. Drevet, S. Pinkasfeld, F. Ducancel, J. C. Boulain, and A. Menez. 1995. Genetic engineering of snake toxins. The functional site of Erabutoxin α, as delineated by site-directed mutagenesis, includes variant residues. *J. Biol. Chem.* 270:9362–9369.

Tzartos, S. J., A. Kokla, S. L. Walgrave, and B. M. Conti-Tronconi. 1988. Localization of the main immunogenic region of human muscle acetylcholine receptor to residues 67–76 of the α-subunit. *J. Neuroimmunol.* 15:185–194.

Unwin, N. 1993. Nicotinic acetylcholine receptor at 9 Å resolution. *J. Mol. Biol.* 229:1101–1124.

Unwin, N. 1995. Acetylcholine receptor imaged in the open state. *Nature.* 373:37–43.

Unwin, N. 1996. Projection structure of nicotinic acetylcholine receptor: distinct conformations of the α subunits. *J. Mol. Biol.* 257:586–596.

Weiner, S. J., P. A. Kollman, D. Case, U. C. Singh, C. Ghio, G. Alagona, S. Profeta, Jr., and P. Weiner. 1984. A new force field for molecular mechanical simulation of nucleic acids and proteins. *J. Am. Chem. Soc.* 106:765–784.

Wo, Z. G., and R. E. Oswald. 1994. Transmembrane topology of two kainate receptor subunits revealed by N-glycosylation. *Proc. Natl. Acad. Sci. USA.* 91:7154–7158.